

ELABELA and an ELABELA Fragment Protect against AKI

Hong Chen,* Lin Wang,[†] Wenjun Wang,[†] Cheng Cheng,* Yu Zhang,* Yu Zhou,[‡] Congyi Wang,[§] Xiaoping Miao,^{||} Jiao Wang,* Chao Wang,* Jianshuang Li,[†] Ling Zheng,[†] and Kun Huang*

*Tongji School of Pharmacy, [§]The Center for Biomedical Research, Tongji Hospital, and ^{||}School of Public Health, Tongji Medical College, Huazhong University of Science and Technology, Wuhan, China; [†]Hubei Key Laboratory of Cell Homeostasis, College of Life Sciences, Wuhan University, Wuhan, China; and [‡]Department of Anesthesiology, Washington University School of Medicine, St. Louis, Missouri

ABSTRACT

Renal ischemia-reperfusion (I/R) injury is the most common cause of AKI, which associates with high mortality and has no effective therapy. ELABELA (ELA) is a newly identified 32-residue hormone peptide highly expressed in adult kidney. To investigate whether ELA has protective effects on renal I/R injury, we administered the mature peptide (ELA32) or the 11-residue furin-cleaved fragment (ELA11) to hypoxia-reperfusion (H/R)-injured or adriamycin-treated renal tubular cells *in vitro*. ELA32 and ELA11 significantly inhibited the elevation of the DNA damage response, apoptosis, and inflammation in H/R-injured renal tubular cells and suppressed adriamycin-induced DNA damage response. Similarly, overexpression of ELA32 or ELA11 significantly inhibited H/R-induced cell death, DNA damage response, and inflammation. Notably, treatment of mice with ELA32 or ELA11 but not an ELA11 mutant with a cysteine to alanine substitution at the N terminus (AE11C) inhibited I/R injury-induced renal fibrosis, inflammation, apoptosis, and the DNA damage response and markedly reduced the renal tubular lesions and renal dysfunction. Together, our results suggest that ELA32 and ELA11 may be therapeutic candidates for treating AKI.

J Am Soc Nephrol 28: 2694–2707, 2017. doi: <https://doi.org/10.1681/ASN.2016111210>

AKI is a potentially fatal syndrome characterized by a rapid decline in kidney function caused by ischemic or toxic injury to renal tubular cells.¹ AKI is one of the most important causes of ESRD,^{2,3} with no viable therapeutics currently available.⁴ Renal ischemia-reperfusion (I/R) injury is the most common cause of AKI.^{5,6} The pathologic process of renal I/R injury involves inflammation and apoptosis.^{1,7} Immuno- or pharmacologic strategies that inhibit inflammatory reaction through suppressing generations of proinflammatory cytokines or inhibit apoptosis effectively protect kidney from acute I/R injury.^{5,8,9}

DNA damage, such as apoptosis-associated DNA cleavage in renal tubular cells, occurs in renal I/R injury.^{10,11} On DNA damage, cells activate a network of signaling pathways known as DNA damage response (DDR) that initiate with the activation of sensors, including ataxia telangiectasis mutated

(ATM) and ataxia telangiectasis and Rad3 related (ATR) protein kinases.^{12,13} ATM and ATR phosphorylate mediators, which further recruit transducers, such as checkpoint kinase 1 and 2 (Chk1/2), to phosphorylate effectors and regulate DNA repair, cell cycle arrest, and cell death.^{14,15} Ser¹³⁹-phosphorylated H2A.X is a hallmark of DNA damage.^{16,17}

Received November 15, 2016. Accepted April 9, 2017.

Published online ahead of print. Publication date available at www.jasn.org.

Correspondence: Prof. Kun Huang, Tongji School of Pharmacy, Huazhong University of Science and Technology, 13th Hangkong Road, Wuhan, China 430030. Email: kunhuang2008@hotmail.com

Copyright © 2017 by the American Society of Nephrology

ELABELA (ELA; also known as toddler or apela) is a newly identified 32-residue peptide.¹⁸ ELA is highly conserved among species, implicating its essential physiologic functions.^{18,19} ELA is found as an early endogenous ligand for apelin receptor (APJ), a member of the G protein-coupled receptor superfamily, in several tissues.¹⁸ We previously showed that apelin, an endogenous ligand for APJ, protects against renal I/R injury⁵; we thus wonder whether ELA also has renoprotective roles. In ELA32, there are two potential furin cleavage sites characterized by conserved diarginines,¹⁸ suggesting that ELA32 may coexist with its cleaved fragments *in vivo*.

Here, we assessed the effects of ELA32 and its shortest furin-cleaved fragment ELA11 (ELA [22–32]) (Figure 1A) on the hypoxia-reperfusion (H/R)-injured renal tubular cells and the renal I/R-injured mice. Cell apoptosis, inflammation,

DDR, tubular lesions, and renal function were examined. Renoprotective effects of ELA32 and ELA11 were observed.

RESULTS

Apela Is Decreased after Renal I/R Injury

To examine the susceptibility of ELA32 to proteolytic cleavage, ELA32 was incubated with furin, and generation of ELA11 was observed by mass spectrometry (data not shown). The mRNA levels of *Apela* (encoding ELA), *Apln* (encoding apelin), and *Aplnr* (encoding APJ) were examined in a variety of tissues from fetal and adult mice. Consistent with a previous report,²⁰ *Aplnr* was detected in diverse tissues of fetal and adult mice (Figure 1B). A high level of *Apln* was detected in brain and lung, whereas *Apela* was detected at a high level in kidneys of fetal and adult mice (Figure 1B). ELA was predominantly expressed in renal tubular epithelial cells, especially on the lumen side of the tubules, with very little glomerular staining (Supplemental Figure 1); staining on the collecting ducts was also observed (data not shown). These data implicate that ELA may play a critical role in kidney.

To assess whether ELA is involved in renal I/R injury, the mRNA level of ELA was examined, and markedly decreased *Apela* was observed in the kidneys of I/R-injured mice (Figure 1C). Because the *Apela* sequence of *Rattus* is not available in database, the protein level of ELA was examined in NRK-52E cells (a rat renal tubular cell line) by immunofluorescence staining. ELA was colocalized with TGN38 (Figure 1D), a trans-Golgi marker, as previously reported.¹⁸ Consistent with *in vivo* results, ELA level was significantly reduced after H/R injury (Figure 1D).

ELA32 and ELA11 Suppress H/R-Induced Inflammation, DDR, and Apoptosis in Cultured Renal Tubular Cells

Renoprotective effect of ELA32 and ELA11 at different dosages on the H/R-injured NRK-52E cells was investigated (Figure 2A). Low dosage (300 pM) of ELA32 and ELA11 significantly inhibited the H/R-induced loss of cell viability, whereas higher dosages (3 and 30 nM) also showed similar effects by MTT assay (Supplemental Figure 2A). Thus, 300 pM ELA was used in most experiments.

The mRNA levels of inflammatory and fibrotic genes (*Il6*, *Icam1*, *Tnfa*, and *Tgfb1*)

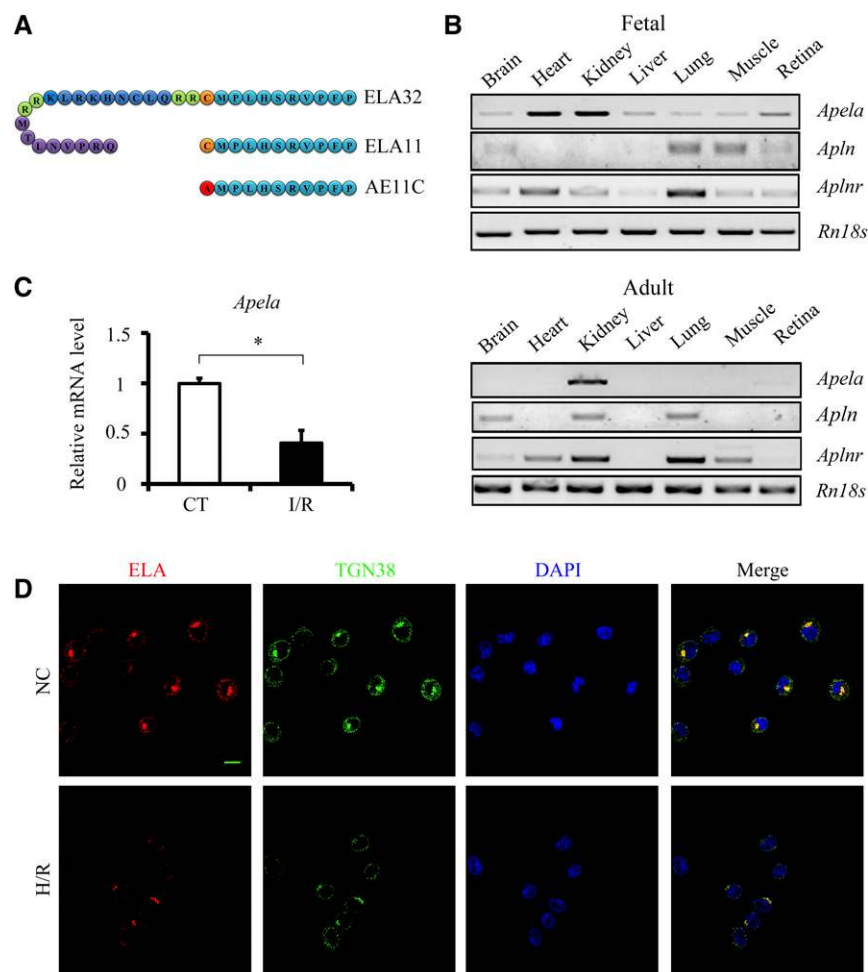


Figure 1. ELA level is downregulated after renal I/R injury *in vivo* and *in vitro*. (A) Sequences of ELA peptides used in this study. (B) RT-PCR results of *Apela*, *Apln*, *Aplnr*, and *Rn18s* in different tissues of fetal and adult mice. (C) qPCR results of *Apela* in the kidneys of different experimental groups ($n=3-4$ per group). CT, noninjured mice. (D) Representative images of ELA (red), TGN38 (green), and 4,6-diamidino-2-phenylindole (DAPI; blue) staining in NRK-52E cells. NC, noninjured cells. Scale bar, 10 μm. * $P<0.05$.

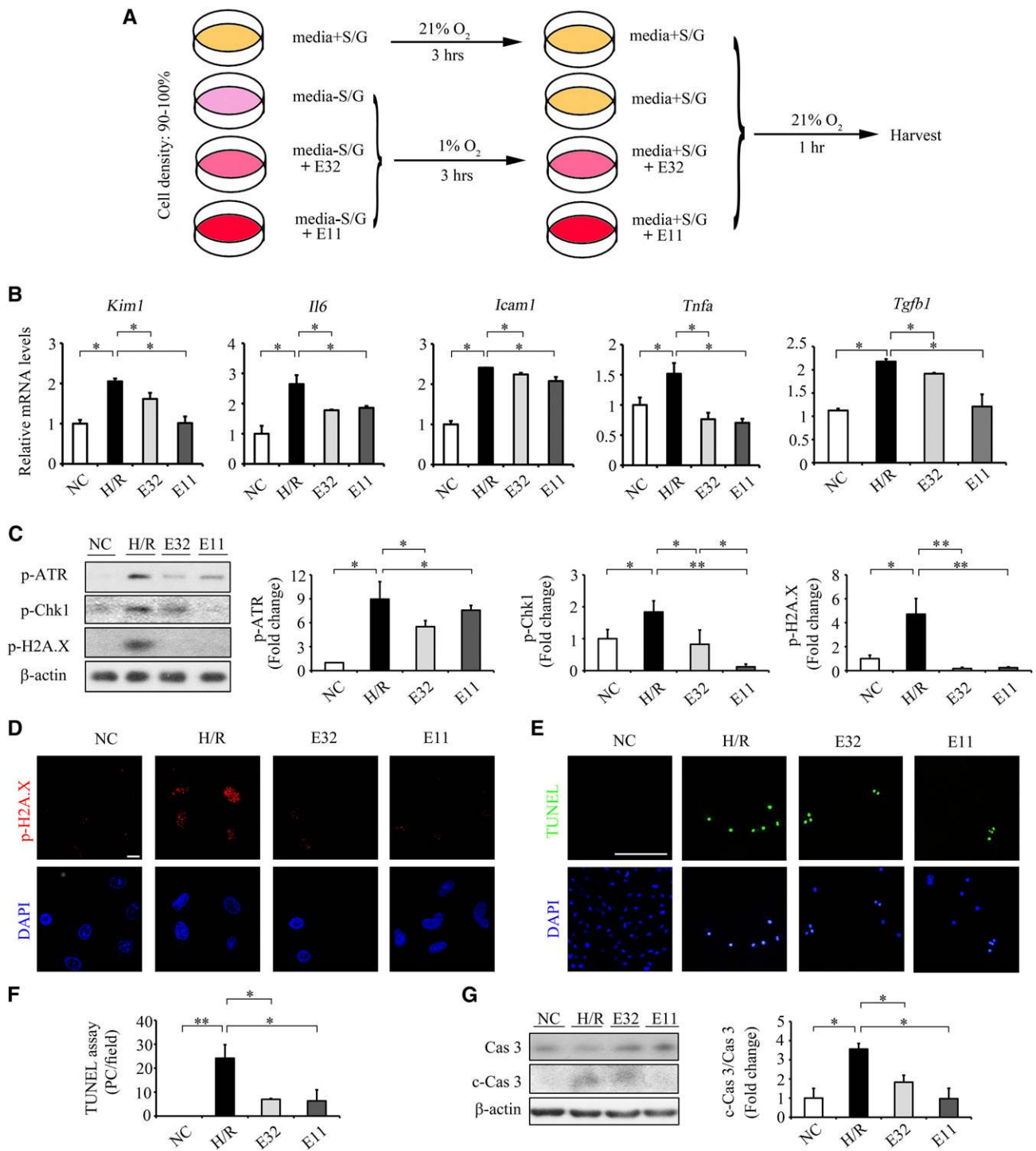


Figure 2. ELA32 and ELA11 treatments suppress H/R injury–induced inflammation, DNA damage, and apoptosis in cultured renal tubular cells. (A) Experimental design chart of H/R. S, serum; G, Glucose. (B) qPCR results of *Kim1*, *Il6*, *Icam1*, *Tnfa*, and *Tgfb1* in different experimental groups. (C) Representative Western blots (left panel) with densitometric quantitative results (right panel) of p-ATR, p-Chk1, p-H2A.X, and β -actin in different experimental groups. (D) Representative images of p-H2A.X in different groups. Scale bar, 10 μ m. (E) Representative images of TUNEL assay and (F) quantitative results of TUNEL-positive cells in different experimental groups. Scale bar, 100 μ m. (G) Representative Western blots (left panel) with densitometric quantitative results (right panel) of caspase3, c-Cas3, and β -actin in different experimental groups. Each experiment was performed in duplicate or triplicate and repeated at least three times. A representative result is shown. DAPI, 4,6-diamidino-2-phenylindole; E11, 300 pM ELA11-treated H/R-injured cells; E32, 300 pM ELA32-treated H/R-injured cells; NC, noninjured cells; PC, positive cells. * P <0.05; ** P <0.01.

and kidney injury marker (*Kim1*) were significantly elevated in H/R-injured NRK-52E cells (Figure 2B). ELA32 and ELA11 significantly inhibited H/R-induced increases in *Kim1* and inflammatory and fibrotic genes in injured cells (Figure 2B).

DDR and apoptosis-associated DNA damage occurred during AKI.^{10,11} The levels of p-ATR, p-Chk1, and p-H2A.X were markedly increased in H/R-injured cells, whereas ELA32 or ELA11 significantly inhibited such upregulation, with ELA11 showing greater inhibitory effect on p-Chk1 (Figure 2C). Moreover, ELA32 and ELA11 also suppressed H/R-induced upregulation of p-H2A.X staining (Figure 2D). Higher dosages of ELA32 and ELA11 (3 and 30 nM) also showed similar effects on the H/R-induced overexpression of p-H2A.X (Supplemental Figure 2, B and C).

Terminal deoxynucleotidyl transferase-mediated digoxigenin-deoxyuridine nick-end labeling (TUNEL) assay detects DNA double- and single-strand breaks, the hallmark of apoptosis. The number of TUNEL⁺ cells was dramatically increased in H/R-injured NRK-52E cells and significantly reduced by ELA32/ELA11 treatment (Figure 2, E and F). Cleavage of caspase 3 (c-Cas3) activates the caspase-dependent apoptosis and represents the execution stage of cell death.²¹ Compared with normoxia cultured cells, the c-Cas3 level was markedly increased in H/R-injured NRK-52E cells, whereas ELA32/ELA11 treatment significantly downregulated its level (Figure 2G).

We compared the protective effects of ELA32, ELA11, and apelin-13 (Supplemental Figure 3A). All three peptides at 300 pM and a combination of 150 pM either ELA32 or ELA11 with 150 pM apelin-13 showed similar protective effects on cell viability, whereas a combination of either 300 pM ELA32 or ELA11 with equimolar apelin-13 showed significantly better effect on cell viability (Supplemental Figure 3A). Meanwhile, 300 pM either ELA32 or ELA11 did not inhibit the H/R-induced elevations of H3K4me2 and H3K79me1 (Supplemental Figure 3B).

Overexpressing ELA or Its 11-Residue Fragment Suppresses H/R Injury-Induced Inflammation, DNA Damage, and Apoptosis in Cultured Renal Tubular Cells

Overexpression of ELA32-GFP or ELA11-GFP in NRK-52E cells (Supplemental Figure 4) significantly inhibited H/R-induced upregulation of inflammatory genes, including *Tnfa*, *Vcam1*, *Mcp1*, and *Il6*, with ELA11-GFP also significantly suppressing *Icam1* (Figure 3A). Furthermore, overexpression of ELA11-GFP and ELA32-GFP significantly increased the viability of H/R-injured NRK-52E cells, with ELA11-GFP showing greater effects (Figure 3B).

Overexpression of ELA32-GFP and ELA11-GFP significantly suppressed H/R-induced increases in p-ATR, p-Chk1, and p-H2A.X levels (Figure 3C) and significantly suppressed H/R-induced increases in c-Cas3 and cleaved poly(ADP-ribose) polymerase-1 (PARP-1), a key substrate of caspase 3.²¹ ELA11-GFP showed greater inhibitory effects on H/R-induced p-ATR, p-H2A.X, and c-Cas3 (Figure 3, C and D).

ELA32 and ELA11 Suppress DDR in Adriamycin-Stimulated Renal Tubular Cells

To investigate whether ELA32 and ELA11 protect renal cells from additional DNA damage stresses, we examined their effects on NRK-52E cells treated with adriamycin (ADR), a topoisomerase II inhibitor that also acts as a nephrotoxin.²² ADR significantly activated DDR, whereas ELA32/ELA11 significantly suppressed ADR-induced upregulation of p-ATR and p-Chk1 (Figure 4, A and B). ELA11 also significantly reduced ADR-induced upregulation of p-H2A.X (Figure 4, A and C). As expected, ELA32 and ELA11 suppressed the ADR-induced loss of cell viability, elevation of c-Cas3, and cleaved PARP-1 (Figure 4, D and F).

Despite its renal toxicity, ADR is used as a chemotherapeutic drug for acute leukemia.^{23,24} Because ELA peptides inhibit ADR-induced DDR in renal cells, we tested whether ELAs interfere with the efficacy of ADR to induce cell death in leukemia cells. ELA32/ELA11 showed no effect on ADR-induced downregulation of cell viability of three leukemia cell lines (NB4, K562, and THP-1) (Supplemental Figure 5), suggesting that the renoprotective effects of ELAs do not interfere with the antileukemia efficacy of ADR.

The Renal Protection Function of ELAs May Be APJ Independent

As an APJ ligand, ELA has been reported to inhibit cAMP production.^{20,25,26} However, the cAMP level was not significantly changed in NRK-52E cells after ELA32 and ELA11 treatments under normal conditions (Figure 5A). The increased cAMP level in ELA11-treated H/R-injured NRK-52E cells indicates that ELA11 may bind to other receptor(s) (Figure 5B).

Ligand-induced receptor endocytosis is a typical cellular response of G protein-coupled receptor,²⁷ and the effect of ELA peptides on APJ endocytosis was examined using APJ-EGFP-transfected HEK293 cells. APJ mainly localized on the cell surface of untreated HEK293 cells (Figure 5C). No obvious APJ endocytosis (shown by intracellular dot-like vesicles) was observed in cells treated with 300 pM peptides for 60 minutes (Figure 5C). Under higher concentrations of ELA peptides (3 or 30 nM) for 60 minutes, endocytosis was observed in ELA32-treated cells but was not observed in ELA11-treated cells (Figure 5C). When concentration was increased to 0.3 or 3 μ M, both peptides caused endocytosis at 30 minutes post-treatment (Figure 5C). Consistently, phosphorylation of extracellular signal-regulated kinase (ERK), a downstream signaling of APJ activation,²⁰ was increased under the treatments of higher concentrations of ELAs but not 300 pM ELA (Supplemental Figure 6).

To further investigate whether APJ is involved in the protective effects of ELAs on H/R injury, *Ap1nr* was knocked down (KD) by siRNA in NRK-52E cells (Supplemental Figure 7A). KD of APJ had no obvious effect on cell viability under normal or H/R conditions (Figure 5D, Supplemental Figure 7B). ELA (0.3–30 nM) neither altered cAMP level (Supplemental

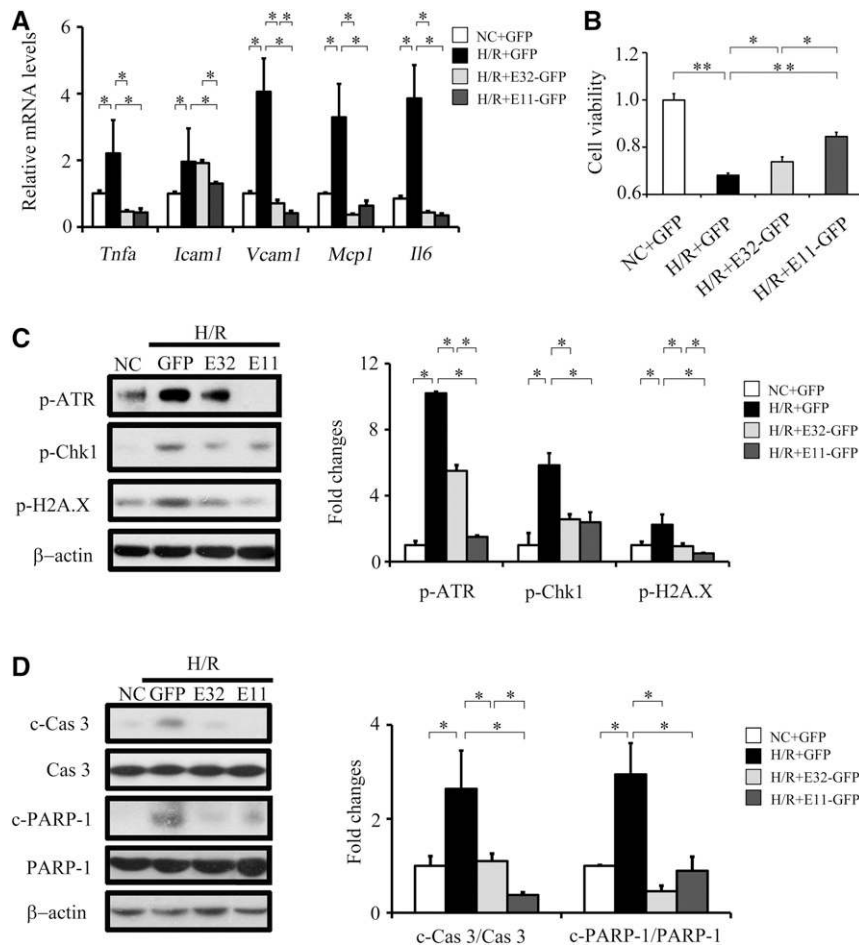


Figure 3. Overexpression of E32-GFP and E11-GFP inhibits H/R injury–induced DNA damage, apoptosis, and inflammation in cultured renal tubular cells. (A) qPCR results of *Tnfa*, *Icam1*, *Vcam1*, and *Il6* in different experimental groups. (B) Relative cell viability measured by MTT assay. (C) Representative Western blots (left panel) with densitometric quantitative results (right panel) of p-ATR, p-Chk1, p-H2A.X, and β-actin in different experimental groups. (D) Representative Western blots (left panel) with densitometric quantitative results (right panel) of caspase3, c-Cas3, PARP-1, c-PARP-1, and β-actin in different experimental groups. Each experiment was performed in duplicate or triplicate and repeated at least three times. A representative result is shown. E11-GFP, cells transfected with the E11-GFP plasmid and cultured under H/R condition; E32-GFP, cells transfected with the E32-GFP plasmid and cultured under H/R condition; H/R+GFP, cells transfected with the pRK-GFP plasmid and cultured under H/R condition; NC, cells transfected with the pRK-GFP plasmid and cultured under normal condition. * $P < 0.05$; ** $P < 0.01$.

Figure 7C) nor changed p-ERK level (data not shown) in APJ KD cells. Surprisingly, both peptides (0.3–30 nM) evidently enhanced cell viability (Figure 5D) and inhibited p-H2A.X level (Supplemental Figure 7D) in H/R-injured APJ KD cells. ELA32 significantly inhibited the H/R-induced increases in *Mcp1* and *Il6* levels, whereas ELA11 significantly inhibited the *Mcp1* level in APJ KD cells (Figure 5E).

ELA Protects Kidney from I/R Injury–Induced Functional and Morphologic Changes

To confirm the H/R injury protection effects observed *in vitro*, we performed *in vivo* study using a mouse renal I/R model (Figure 6A). To evaluate the role of the N-terminal cysteine, an ELA11 mutant was generated (cysteine to alanine; AE11C) (Figure 1A). Because the mRNA levels of *Kim1* and *Il6* were

significantly higher on day 3 than day 1 after the I/R injury (Supplemental Figure 8A), a similar conclusion was drawn from the morphologic examination (Supplemental Figure 8B); therefore, the renal function, pathologic lesions, and biochemical abnormalities were examined at day 3 after the injury.

Three days after renal I/R injury, serum creatinine, 24-hour urine volume, proteinuria, urine creatinine, and nitrogen levels were significantly elevated (Supplemental Table 1), indicating marked loss of renal function. Meanwhile, ELA32 and ELA11 but not AE11C suppressed I/R injury–induced elevation of these renal functional parameters (Supplemental Table 1). The serum BUN level showed no significant difference among groups (data not shown). Compared with noninjured kidneys, I/R injury led to severe tubular damage as evidenced by

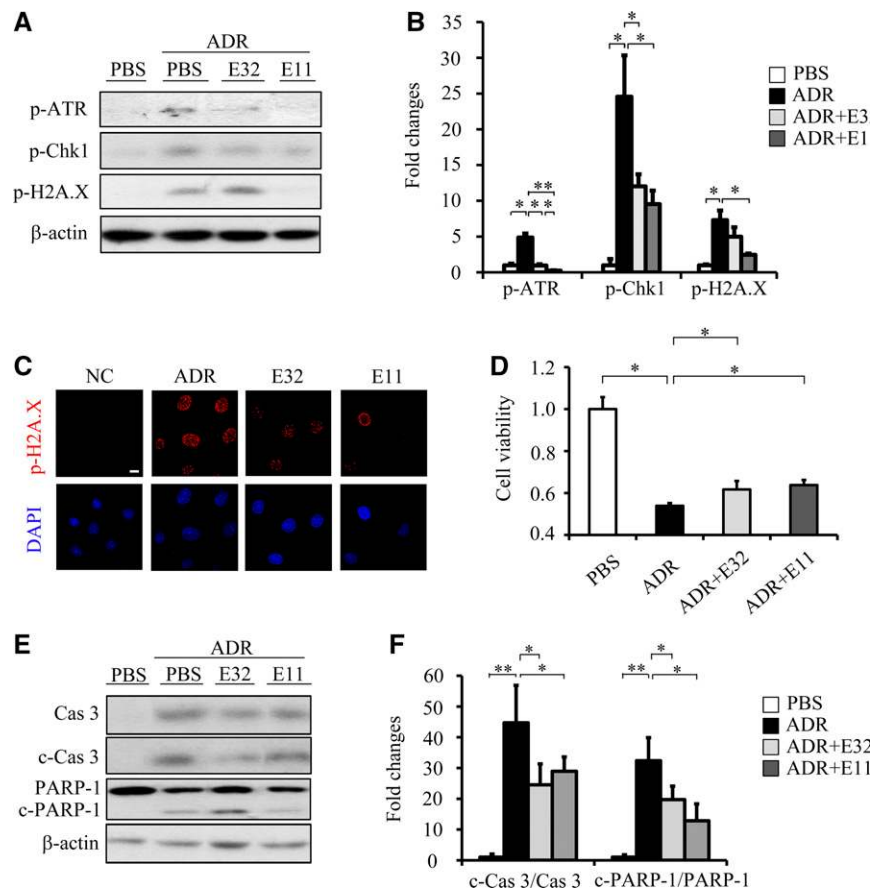


Figure 4. ELA32 and ELA11 treatments inhibit ADR-induced DNA damage in cultured renal tubular cells. (A) Representative Western blots with (B) densitometric quantitative results of p-ATR, p-Chk1, p-H2A.X, and β -actin in different experimental groups. (C) Representative images of p-H2A.X staining in different groups. Scale bar, 10 μ m. (D) Relative cell viability measured by MTT assay. (E) Representative Western blots with (F) densitometric quantitative results of caspase3, c-Cas3, PARP-1, c-PARP-1, and β -actin in different experimental groups. Each experiment was performed in duplicate or triplicate and repeated at least three times. A representative result is shown. ADR, 0.5 μ M ADR-treated NRK-52E cells; DAPI, 4,6-diamidino-2-phenylindole; E11, 300 pM ELA11-treated ADR-injured cells; E32, 300 pM ELA11-treated ADR-injured cells; NC, noninjured cells; PBS, PBS-treated NRK-52E cells. * P <0.05; ** P <0.01.

widespread tubular necrosis, cast formation, and tubular cells denudation (Figure 6, B and C). ELA32 and ELA11 but not AE11C significantly improved the pathologic scores in injured kidneys (Figure 6, B and C).

Increased macrophage infiltration was found in I/R-injured kidneys shown by panmacrophage marker F4/80 staining; administration of ELA32 and ELA11 but not AE11C significantly inhibited I/R-induced macrophage infiltration (Figure 6, D and E). Consistently, various inflammatory gene (*Il6*, *Mcp1*, and *Il8*) levels were significantly increased in the kidneys of I/R-injured mice (Figure 6F); ELA32 and ELA11 markedly inhibited *Mcp1* and *Il8* levels, whereas ELA11 also inhibited *Il6* level, and AE11C showed no effects (Figure 6F).

Fibrosis markers, such as collagen deposition (Masson staining), α -smooth muscle actin, and vimentin, were further analyzed. ELA32 and ELA11 protected the I/R-injured mice from developing overt fibrosis (Figure 6G), whereas AE11C showed no obvious effects (Figure 6G). Consistently, the

mRNA levels of fibrotic genes (*Vimentin*, *Tgfb1*, *Fibronectin*, and *Collagen1a*) were markedly elevated after renal I/R injury (Figure 6H); ELA32 and ELA11 treatments significantly inhibited the levels of *Tgfb1*, *Fibronectin*, and *Collagen1a*, whereas ELA11 also decreased *Vimentin*, and AE11C showed no obvious effects (Figure 6H). Because AE11C showed no improvement on renal I/R injury, its effect was not studied further.

ELAs Suppress Renal I/R Injury–Induced DDR and Apoptosis

The expressions of p-ATR, p-Chk1, and p-H2A.X were barely detectable in the kidneys of noninjured mice but dramatically elevated after I/R injury (Figure 7, A and B). ELA11 and ELA32 significantly suppressed the I/R-induced elevation of p-Chk1 and p-H2A.X in injured kidneys (Figure 7, A and B). Compared with ELA32, ELA11 showed stronger inhibition on I/R injury–induced p-ATR and p-Chk1 levels (Figure 7, A and B). Meanwhile, ELA11 and ELA32 also suppressed I/R

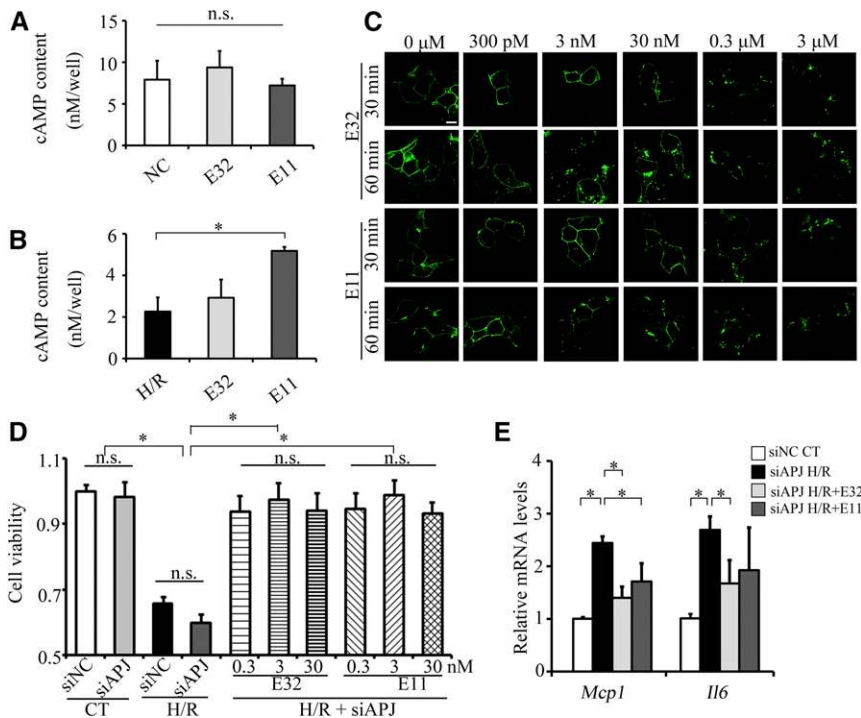


Figure 5. ELA may not bind to APJ in renal I/R injury. cAMP assay of ELA32 and ELA11 in (A) normoxia and (B) H/R-injured NRK-52E cells. (C) Internalization of APJ by ELA32 and ELA11 in HEK293 cells. Scale bar, 10 μ m. (D) Cell viability of different groups. (E) qPCR results of *Mcp1* and *Il6* in different experimental groups. CT, noninjured mice; NC, noninjured cells. * $P < 0.05$.

injury-induced upregulation of p-H2A.X staining in renal epithelial cells (Figure 7C). Compared with noninjured kidneys, elevated c-Cas 3 and increased number of TUNEL⁺ cells were found in the kidneys of I/R-injured mice, which were markedly attenuated by ELA32 or ELA11 treatment (Figure 7, D and F).

ELA11 Inhibits the Injury-Induced Elevation of Autophagy

Autophagy has been reported to play an important role in renal I/R injury and diabetes.^{28–30} The levels of Atg5, Atg7, Atg12, and LC3B-II were significantly increased in the kidneys of I/R-injured mice, which were significantly inhibited by ELA 11 but not ELA32 (Figure 8, A and B). Consistently, ELA11 not only significantly decreased H/R-induced elevations of Atg5 and LC3B-II levels (Figure 8C) but also, inhibited the rapamycin-induced loss of cell viability (Figure 8D) and autophagy in NRK-52E cells (Figure 8, E and F).

DISCUSSION

Among various etiologies of hospital-acquired AKI, I/R injury is the leading cause associated with high mortality rate,^{3,6} and an optimal therapy for AKI is still lacking. Here, we found that ELA32 and ELA11 both have renoprotective effects on I/R injury, with ELA11 showing even better effects. To our

knowledge, this is the first report about this endogenous ELA peptide, which previously has only been shown to involve in heart development and stem cell maintenance,^{18,31} also functioning in kidney injury.

Consistent with a previous report,²⁰ *Apela* is highly expressed in the kidneys of fetal and adult mice (Figure 1). The promoter and the enhancer of *ELA* have been shown to have multiple binding sites for master transcription factors involved in kidney development, including *Tcfcp2l1*, *Myc*, *Nanog*, *Sox2*, and *Oct4*,^{31,32} which might explain the high expression level of ELA in the kidney.

DNA damage, such as accumulation of apoptosis-associated DNA cleavage in renal tubular cells, occurs in the I/R-injured kidney.^{10,33} Other than I/R injury, other AKI models, such as cisplatin injection, also activate the DDR signaling pathway that leads to upregulation of apoptotic genes, therefore causing tubular cell death and renal damage.^{34–36} Thus, activation of the DDR signaling pathway may represent a common pathway that causes renal cell damage in AKI. Lovastatin and cilastatin, two well known clinical prescriptions to treat renal damage, also work as DDR inhibitors to

protect cells from cisplatin-induced stress.^{37,38} Consistently, we found that ELAs inhibited I/R- or H/R-induced activation of the DDR signaling pathway (Figures 2, 3, and 7).

I/R injury triggers inflammatory responses and subsequently attracts neutrophil and macrophage infiltration into the tubulointerstitium, leading to kidney damage and development of fibrosis.^{39–41} The crucial roles of inflammatory genes in renal I/R injury have been suggested.^{8,41} Here, ELA32 and ELA11 not only significantly suppressed inflammatory molecules in H/R-injured cells and I/R-injured kidneys (Figures 2, 3, and 7) but also, inhibited macrophage infiltration in the latter (Figure 6).

ELA and apelin are both endogenous APJ agonists. Recently, Hsueh and coworkers²⁰ elegantly compared the effects of ELA32 and apelin-13 on p-ERK level and fluid homeostasis. Although both peptides bind APJ with similar affinity, compared with apelin-13, ELA32 at same dosage is more potent in stimulating ERK phosphorylation and regulating diuresis and water intake in rats.²⁰ These data indicate that, other than binding to APJ, functional difference between two peptides may exist. Here, we found that, at lower dosage (300 pM), apelin-13 and ELAs have comparable effects on H/R injury (Supplemental Figure 3). Synergistic protection against H/R-induced loss of cell viability was suggested by combining ELA32 or ELA11 with apelin-13 (Supplemental Figure 3A). Although apelin-13 protects against renal I/R injury through

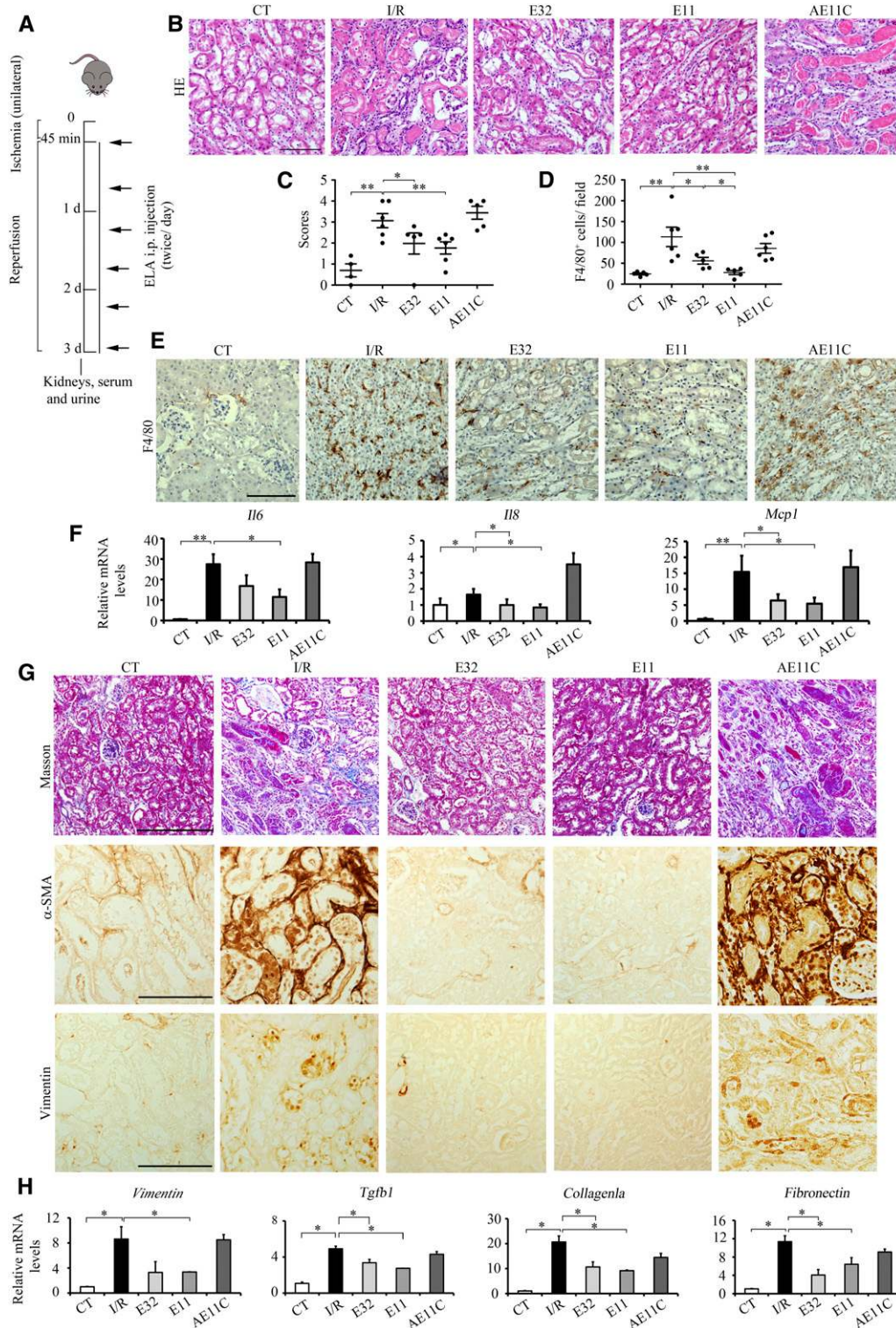


Figure 6. ELA treatments inhibit I/R injury–induced morphologic changes, inflammation, and fibrosis. (A) Experimental design. (B) Representative images of hematoxylin and eosin (HE) and (C) quantitative results of renal damage score in different experimental groups. (D) Quantitative results of F4/80 staining and (E) representative images of F4/80 in different experimental groups. (F) qPCR results of *Mcp1*, *Il6*, and *Il8* in different experimental groups. (G) Representative images of Masson, α -smooth muscle actin (α -SMA), and vimentin staining in different experimental groups. (H) qPCR results of *Vimentin*, *Tgfb1*, *Fibronectin*, and *Collagen1a* in different experimental groups. AE11C, AE11C-treated I/R-injured mice ($n=3-7$ per group); CT, noninjured mice; E11, ELA11-treated I/R-injured mice ($n=3-7$ per group); E32, ELA32-treated I/R-injured mice ($n=3-7$ per group). Scale bar, 100 μ m. * $P<0.05$; ** $P<0.01$.

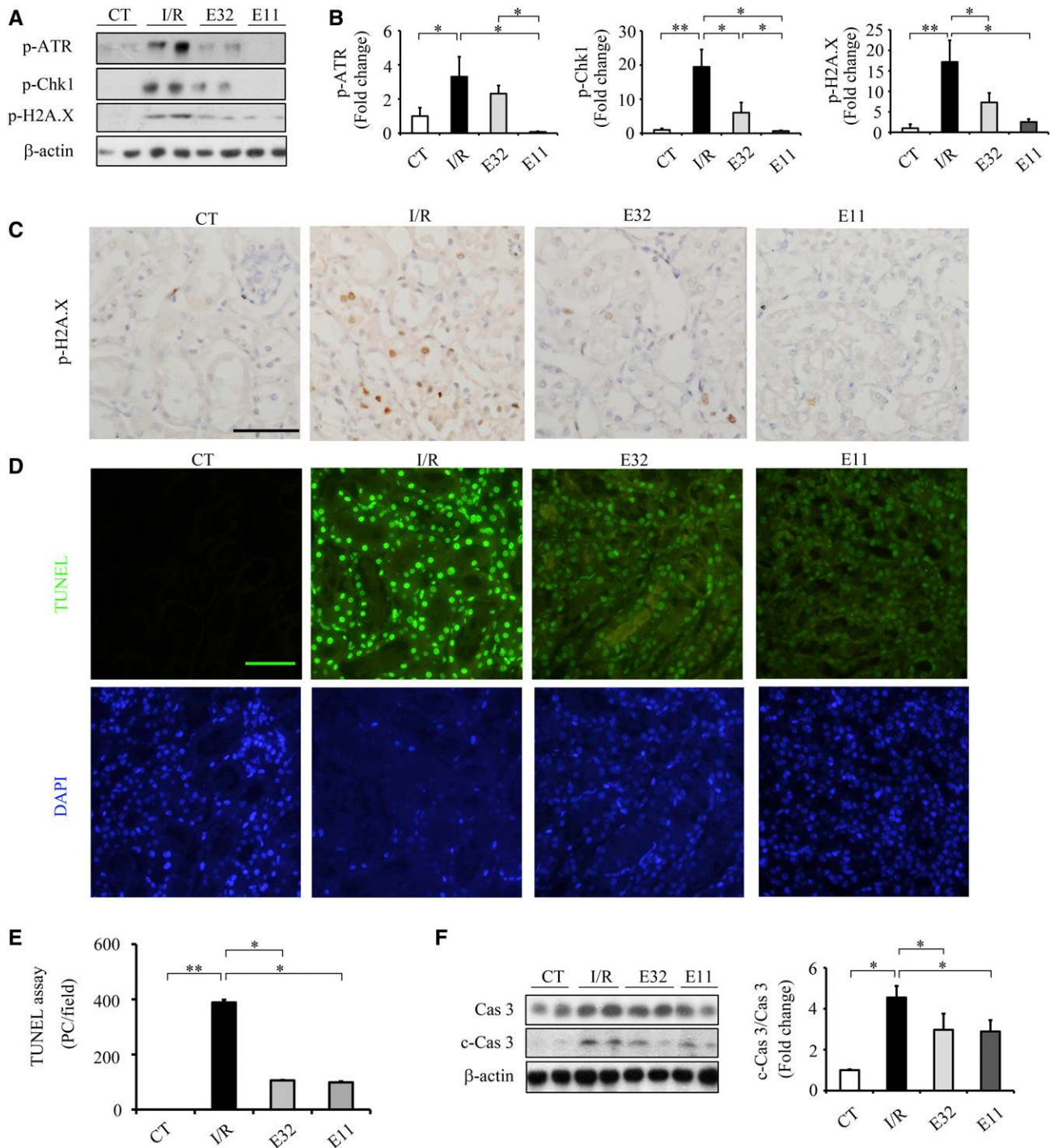


Figure 7. ELA treatments suppress I/R injury–induced DDR and apoptosis in the kidneys. (A) Representative Western blots with (B) densitometric quantitative results of p-ATR, p-Chk1, p-H2A.X, and β-actin in different experimental groups. (C) Representative images of p-H2A.X (brown) in different groups. (D) Representative images of TUNEL assay and (E) quantitative results of TUNEL-positive cells in different experimental groups. (F) Representative Western blots (left panel) with densitometric quantitative results (right panel) of caspase3, c-Cas3, and β-actin in different experimental groups. CT, noninjured mice; DAPI, 4,6-diamidino-2-phenylindole; E11, ELA11-treated I/R-injured mice (n=3–7 per group); E32, ELA32-treated I/R-injured mice (n=3–7 per group); PC, positive cells. Scale bar, 50 μm. *P<0.05; **P<0.01.

inhibiting TGF-β1 and restoring histone methylation,⁵ ELA inhibits the H/R- or I/R-induced elevation of TGF-β1 and inflammation without altering global histone methylation level

(Figures 2 and 6, Supplemental Figure 3B). These data suggested that there are functional overlaps between apelin-13 and ELAs, whereas specific functions for each peptide may still exist. It will

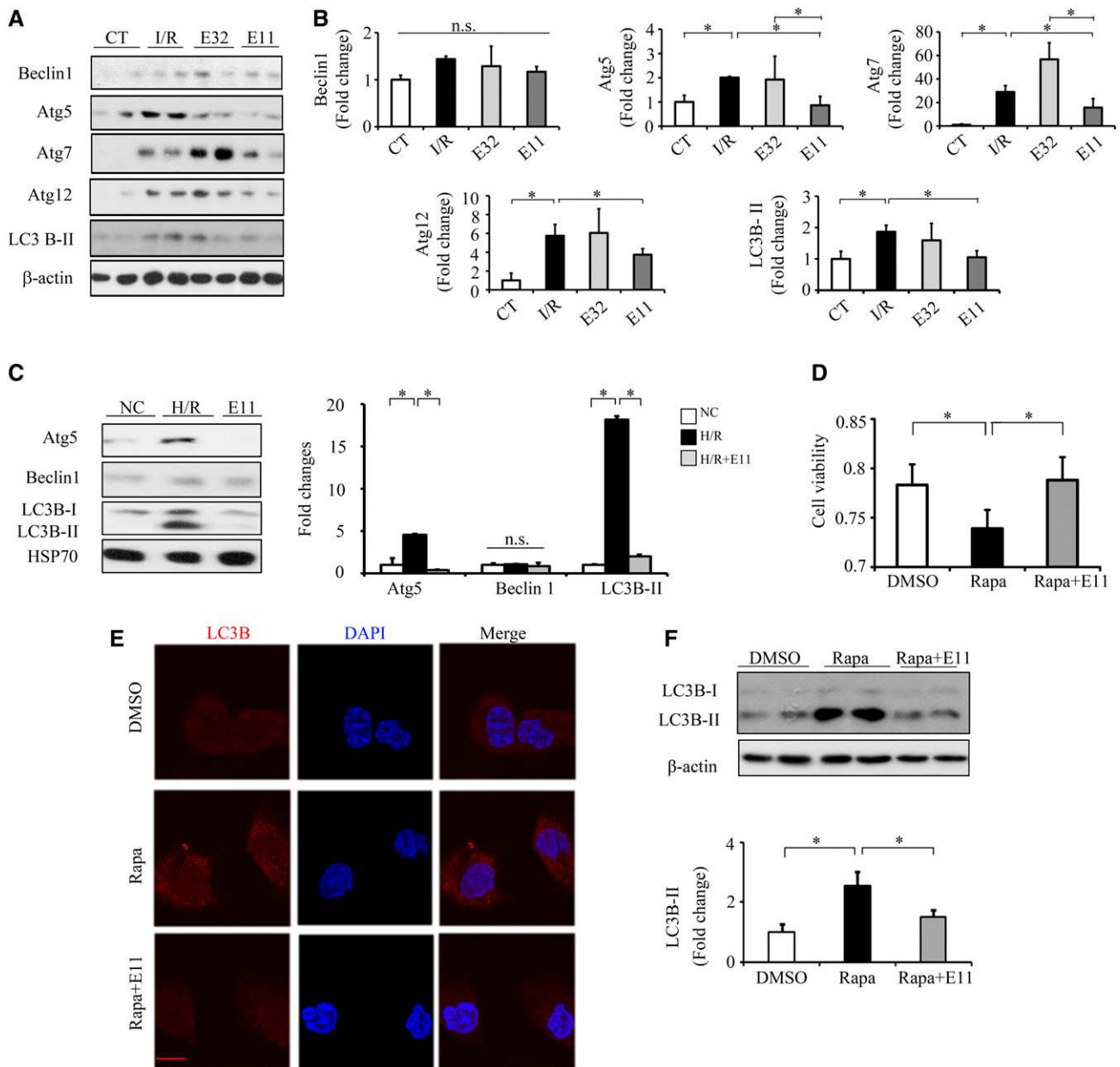


Figure 8. ELA11 treatment suppresses I/R injury–induced autophagy in the kidneys. (A) Representative Western blots with (B) densitometric quantitative results of Atg5, Beclin1, Atg7, Atg12, LC3B-II, and β -actin in different experimental groups. CT, noninjured mice; E11, ELA11-treated I/R-injured mice ($n=3-7$ per group); E32, ELA32-treated I/R-injured mice ($n=3-7$ per group). (C) Representative Western blots with densitometric quantitative results of Atg5, Beclin 1, LC3B-II, and HSP70 in different experimental groups. E11, 300 pM ELA11-treated H/R-injured cells; NC, noninjured cells. (D) Relative cell viability measured by MTT assay in NRK-52E cells treated with rapamycin (Rapa). (E) Representative images of LC3B-II in different groups. DAPI, 4,6-diamidino-2-phenylindole. Scale bar, 10 μ m. (F) Representative Western blots with densitometric quantitative results of LC3B-II and β -actin in different experimental groups. Each experiment was performed in duplicate or triplicate and repeated at least three times. A representative result is shown. DMSO, DMSO-treated NRK-52E cells; Rapa+E11, 300 pM ELA11-treated rapamycin-injured cells. $*P<0.05$.

be of great future interest to explore the effect of combinations of ELAs and apelin-13 on renal injury.

Our results suggest that APJ may not be involved in the renoprotective function of ELAs, at least in cultured renal cells. The activation of APJ downregulates cAMP.^{25,27} In this study,

the cAMP level was not downregulated by ELA32 and ELA11 at the dosages that induce anti-inflammatory and anti-DDRs (Figure 5). Consistent with a previous study,²⁷ higher concentrations of ELA peptides (0.3 and 3 μ M) could induce APJ endocytosis and phosphorylation of ERK, whereas a lower

dosage (300 pM) could not (Figures 5C, Supplemental Figure 6). Other than APJ, there is no other receptor for ELA identified to date. However, the APJ-independent role of ELA32 has been reported previously.^{31,32} *Apela* can act as a regulatory RNA, independent of its protein-coding capacity, to maintain genomic integrity of mouse embryonic stem cells.³² Furthermore, ELA32 acts as an endogenous growth factor to sustain stem cell self-renewal in human embryonic stem cells, which do not express APJ, thus suggesting that an unknown receptor may exist for ELA32.³¹ It is thus of great future interest to identify potential new receptor(s) for ELAs and understand the additional APJ-independent mechanism for ELAs to function.

ELA11 showed better renoprotective effects on I/R or H/R injury compared with ELA32; consistently, endogenous overexpression of ELA11 showed better effect than ELA32 on H/R-induced DDR, apoptosis, and cell viability (Figures 2–4, 6, and 7). Similarly, ELA11 but not ELA32 showed inhibitory effects on I/R-induced autophagy in the kidney (Figure 8). In a comparison study, the cysteine at the N terminus of ELA11 seems critical for its renoprotective functions; biochemical approaches, like alanine or cysteine scanning, will be useful to pinpoint the role of each residue in ELA.^{20,42}

In summary, this study revealed a novel mechanism underlying the anti-inflammatory, antiapoptotic, and antifibrotic actions of ELA peptides, which confers protection against I/R injury in kidneys and cultured renal cells by DDR. All of these suggest that ELA32 and ELA11 may be considered as potential candidates to treat renal I/R injury and AKI.

CONCISE METHODS

Animals and Renal I/R Model

C57BL/6 mice were obtained from the Hubei Animal Laboratory and housed in ventilated microisolator cages with free access to water and food in a temperature-controlled room (22°C ± 2°C). Mice weighing 25 ± 2 g were used and assigned to one of the following groups: CT group, uninjured mice with vehicle administration; I/R group, mice underwent I/R injury with vehicle administration; and I/R+ELA32/ELA11/AE11C group, mice underwent I/R injury with ELA32/ELA11/AE11C treatment. Human ELA32 peptide (>98% purity), QRPVNLTMRRLRKHNLQRRCLMPLHSRVPFP, was purchased from GenScript (Piscataway, NJ); ELA11 (human) and AE11C were chemically synthesized by standard Fmoc strategy and purified to >98% with rp-HPLC as we previously described.⁴³ I/R injury was performed as previously described.⁵ Briefly, mice were anesthetized and underwent midline abdominal incisions with their left renal pedicle bluntly clamped by a clamp for 45 minutes (unilateral renal occlusion). Reperfusion was recovered by removing the clamps. Wounds in abdomens were sutured, and the animals were allowed to recover for 3 days before euthanasia. Control animals were sham operated; 1.2 μmol/kg body wt ELA32, ELA11, or AE11C was subcutaneously administered two times a day (10:00 a.m. and 4:00 p.m.) from the day of I/R injury to the end of the experiment. After

operation of I/R, ELA treatments started. At the same time, the I/R and CT groups received an equal volume of saline solution. Kidneys and serum were harvested 3 days after the I/R injury; one half of the kidney was fixed in freshly prepared 4% paraformaldehyde for IHC, and the other one half was used for Western blots and RNA isolation. All animal experiments were approved by the Committee on Ethics in the Care and Use of Laboratory Animals of the College of Life Sciences, Wuhan University.

Assessment of Renal Function

Twenty-four-hour urine samples were collected in metabolic cages from days 2 to 3 after the I/R injury. Serum levels of creatinine and BUN were analyzed with a Siemens ADVIA 2400 automatic biochemistry analyzer using a creatinine reagent kit (Fuxing Changzheng Medical, Shanghai, China) and a BUN reagent kit (Fuxing Changzheng Medical). Urine levels of nitrogen (BUN), creatinine, and total protein were measured with an Olympus AU2700 automatic biochemistry analyzer using a Urine BUN reagent kit (Fuxing Changzheng Medical), a creatinine reagent kit (Fuxing Changzheng Medical), or a total protein reagent kit (Greatwall Clinical Reagent, Baoding, China) as we previously described.⁴⁴

Renal Histology

Renal sections were stained with hematoxylin and eosin for renal damage examination. Acute tubular necrosis was examined in a double-blind manner, and the degree of renal damage was semiquantitatively evaluated with a scale in which zero represents no abnormality and one, two, three, and four stand for slight (up to 20%), moderate (20%–40%), severe (40%–60%), and total necrosis (affecting >80% of renal parenchyma), respectively.⁵ Masson trichrome staining was performed following the manufacturer's instructions (SBJ Biotechnology, Nanjing, China) for fibrosis examination with aniline blue staining for collagen.

Antibody for ELA Peptide

Mouse polyclonal antibody against ELA was raised from a human C-terminal epitope (KLRKHNLQRRCLMPLHSRVPFP). This antibody was used for immunofluorescence and immunohistochemical staining in this study.

Immunohistochemical Staining

Fixed kidney tissues were embedded in paraffin; 5-μm sections were cut, deparaffinized, and hydrated in graded ethanol series before staining. Immunohistochemical staining was performed as we previously reported.^{45,46} Antigens were retrieved by boiling sections for 5 minutes in 10 mM citric acid solution (pH 6.0) three times. Endogenous peroxidase was blocked by incubation in 3% hydrogen peroxide. The sections were incubated overnight at 4°C with the following primary antibodies: p-H2A.X (ser¹³⁹) (9718P; Cell Signaling Technology), α-smooth muscle actin (A2547; Sigma-Aldrich), vimentin (LV177812; Millipore), F4/80 (sc-52664; Santa Cruz Biotechnology), and ELA. The sections were incubated with the corresponding biotinylated secondary antibodies and sequentially incubated in ABC-Peroxidase Solution (Vector Laboratories), and 3,3'-diaminobenzidine (Beyotime) was used as chromogen. Sections

were lightly counterstained with hematoxylin, dehydrated, and cover slipped.

TUNEL Assay

Sections and cells were detected by TUNEL assay using an In Situ Cell Death Detection Kit (Roche, Mannheim, Germany) as we previously described.^{5,47} Briefly, paraffin-embedded sections were deparaffinized, rehydrated, and antigen retrieved. The next procedures were following the manufacturer's instructions. For *in vitro* experiments, cells were seeded to 12-well plates at a density of 2×10^4 cells per well and cultured overnight. Then, cells were treated with or without ELAs during the hypoxia as well as reperfusion periods. Cells were fixed with 100% methanol at -20°C for 10 minutes and permeabilized with 0.1% Triton X-100 in PBS for 5 minutes. The next procedures were following the manufacturer's instructions. Quantitative results of TUNEL-positive cells were performed as we previously reported.⁵ The pictures of TUNEL-positive cells were obtained by using an Olympus BX60 microscope equipped with a digital CCD.

Cell Culture, *In Vitro* H/R Injury, and Treatments

NRK-52E (a rat tubular epithelia cell line) was cultured in DMEM (Gibco; Life Technologies) plus 5% FBS (PAN-Biotech, Adenbach, Germany) and maintained in a 37°C incubator (Thermo Scientific, Marietta, GA) with humidified atmosphere of 21% O_2 , which was regarded as the normal culture condition. *In vitro* H/R experiments were performed as previously described with slight modifications.^{5,48} At 80% confluence, cells were put into a 37°C incubator under 21% O_2 with the normal media replaced with media lacking glucose and FBS under 1% O_2 , which was regarded as hypoxia. After culturing under the hypoxia condition for 3 hours, cells were returned to the normal culture condition for 1 hour, which was regarded as reperfusion. For ELA treatments, different dosages (300 pM and 3 and 30 nM) of ELA peptides were added to media during the hypoxia as well as reperfusion periods, whereas H/R group or control group received an equal volume of PBS. For induction of DNA damage, 0.5 μM ADR (Sigma-Aldrich) was added to media for 16 hours. For induction of autophagy, 0.5 μM rapamycin (Sigma-Aldrich) was added to media for 12 hours. The siAPJ (rat) was purchased from RiboBio (Guangzhou, China) and added to media at a concentration of 25 pmol for 48 hours.

Plasmid Construction

The human *APELA* cDNA was amplified from genomic cDNA of HEK293 cells by PCR with *EcoRI/XbaI* restriction sites and cloned into a pRK-GFP vector (gift from Hongbing Shu, Wuhan University). *APELA* fragment (E11) was amplified by different primers constructed in the same vector. The human APJ cDNA was amplified from cDNA library by PCR with *EcoRI/NotI* restriction sites and cloned into a pEGFP-N1 vector (gift from Dr. Xiaodong Zhang, Wuhan University). The cDNA inserts of all constructs were confirmed by restriction enzyme digestion and DNA sequencing.

Immunofluorescence Staining

After fixation and blocking with 2% BSA, primary antibodies against ELA (1:200 dilution), p-H2A.X, or LC3B-II were applied to the cells

overnight at 4°C . After washing with PBS three times, the cells were incubated with the appropriate secondary antibody. Cells were covered with 4,6-diamidino-2-phenylindole dye and antifading medium. Imaging was captured with an Olympus FV10-ASV Confocal Microscope (Olympus).

Western Blots

Freshly collected kidney or cultured cells were sonicated in ice-cold RIPA buffer (Beyotime), and protein concentrations were quantitated as previously described^{49,50}; 20–80 μg protein from each sample was separated by SDS-PAGE. The proteins were transferred onto PVDF membranes for immune detection. The list of antibodies used in this study is as follows: p-Chk1 (Ser³⁴⁵; 2348; Cell Signaling Technology), p-ATR (Ser⁴²⁸; 2853; Cell Signaling Technology), caspase3 (9665; Cell Signaling Technology), PARP-1 (C2-10; ENZO), Atg3 (3415p; Cell Signaling Technology), Atg5 (8540p; Cell Signaling Technology), Atg7 (2631p; Cell Signaling Technology), Beclin1 (3495p; Cell Signaling Technology), LC3B (L7543; Sigma-Aldrich), β -actin (A5316; Sigma-Aldrich), H3K4me2 (32356; Abcam), H3K79me1 (39922; Active Motif), and H3 (9715; Cell Signaling Technology). The intensity of the targeted protein band was evaluated using the Quantity One 1-D Analysis Software. Individual protein level was quantitated relative to the β -actin level in the same sample and further normalized to the respective control group, which was set as one.

RNA Isolation and qPCR

Total RNA was isolated from kidneys or cultured cells using RNA^{iso} Plus (TaKaRa Biotechnology, Dalian, China) as we previously reported.⁵¹ Total RNA was reverse transcribed into cDNA using the M-MLV first-strand synthesis system (Invitrogen, Grand Island, NE). The abundance of specific gene transcripts was assessed by qPCR. The sequences of the primers used are listed in Supplemental Table 2. The mRNA level of the targeted gene was quantitated first against the *Rn18s* level from the same sample and then normalized to the noninjured group or the cells transferred with control vector under normal conditions, which was set as one.

cAMP Assay

The cellular cAMP levels were determined with a cAMP-Glo kit (Promega, Madison, WI) following the manufacturer's instructions. Briefly, NRK-52E cells were seeded at 1000 cells per well in 384-well plates coated with poly-D-lysine (BD Bioscience, East Rutherford, NJ). At 80% confluence, medium was removed, and cells were incubated with either ELA32 or ELA11 prepared in induction buffer (serum-free media containing 500 μM isobutyl-1-methylxanthine [Sigma-Aldrich] and 100 μM 4-(3-butoxy-4-methoxy-benzyl) imidazolidone [Sigma-Aldrich]). After induction for 1 hour, the luminescence values were determined using a Synergy HT reader (BioTek, Winooski, VT).

Internalization Assay

HEK293 cells were overexpressing EGFP-tagged APJ for 24 hours and treated with different ELA peptides of different doses (0 and 300 pM, 3 and 30 nM, and 0.3 and 3 μM). Imaging was captured with an Olympus FV10-ASV Confocal Microscope (Olympus, Japan) at different time intervals after treatments.

ELA32 Digestion

Twenty-eight microliters furin digestion buffer (100 mM HEPES, 0.5% Triton X-100, 1 mM CaCl₂, and 1 mM β-mercaptoethanol), 1 μl furin (2 U/ml; Sigma-Aldrich), and 1 μg ELA32 were incubated at 4°C for 16 hours or 30°C for 1 and 3 hours. The samples were analyzed by MALDI-TOF.

Cell Viability Assay

Cells were plated at 4000–5000 cells per well. At 80% confluence, cells under the H/R injury were treated with or without different ELA peptides or transfected with different overexpressing plasmids as we previously reported.⁵² Then, 10 μl MTT (5 mg/ml; Sigma-Aldrich) was added to each well. After 4 hours, medium was removed, DMSO was added, and absorbance measured at 490 nm was normalized to the respective control group, which was arbitrarily set as one.

Statistical Analyses

The data were expressed as means ± SEM. Statistical significance was determined by analyzing the data with the nonparametric Kruskal–Wallis test followed by the Mann–Whitney test. Differences were considered statistically significant with $P < 0.05$.

ACKNOWLEDGMENTS

This work was supported by Natural Science Foundation of China grants 31471208, 31500941, and 31671195; China Postdoctoral Science Foundation–funded projects 2015M572149 and 2016T90692; the Front Youth Program of Huazhong University of Science and Technology; and Natural Science Foundation of Hubei Province grants 2014CFA021 and 2016CFA012.

DISCLOSURES

None.

REFERENCES

1. Arai S, Kitada K, Yamazaki T, Takai R, Zhang X, Tsugawa Y, Sugisawa R, Matsumoto A, Mori M, Yoshihara Y, Doi K, Maehara N, Kusunoki S, Takahata A, Noiri E, Suzuki Y, Yahagi N, Nishiyama A, Gunaratnam L, Takano T, Miyazaki T: Apoptosis inhibitor of macrophage protein enhances intraluminal debris clearance and ameliorates acute kidney injury in mice. *Nat Med* 22: 183–193, 2016
2. Molitoris BA: Therapeutic translation in acute kidney injury: The epithelial/endothelial axis. *J Clin Invest* 124: 2355–2363, 2014
3. Susantitaphong P, Cruz DN, Cerda J, Abulfaraj M, Alqahtani F, Koulouridis I, Jaber BL; Acute Kidney Injury Advisory Group of the American Society of Nephrology: World incidence of AKI: A meta-analysis. *Clin J Am Soc Nephrol* 8: 1482–1493, 2013
4. Kaushal GP, Shah SV: Challenges and advances in the treatment of AKI. *J Am Soc Nephrol* 25: 877–883, 2014
5. Chen H, Wan D, Wang L, Peng A, Xiao H, Petersen RB, Liu C, Zheng L, Huang K: Apelin protects against acute renal injury by inhibiting TGF-β1. *Biochim Biophys Acta* 1852: 1278–1287, 2015
6. Lameire NH, Bagga A, Cruz D, De Maeseeneer J, Endre Z, Kellum JA, Liu KD, Mehta RL, Pannu N, Van Biesen W, Vanholder R: Acute kidney injury: An increasing global concern. *Lancet* 382: 170–179, 2013
7. Rabb H, Griffin MD, McKay DB, Swaminathan S, Pickkers P, Rosner MH, Kellum JA, Ronco C; Acute Dialysis Quality Initiative Consensus XIII Work Group: Inflammation in AKI: Current understanding, key questions, and knowledge gaps. *J Am Soc Nephrol* 27: 371–379, 2016
8. Xu MJ, Feng D, Wang H, Guan Y, Yan X, Gao B: IL-22 ameliorates renal ischemia-reperfusion injury by targeting proximal tubule epithelium. *J Am Soc Nephrol* 25: 967–977, 2014
9. Jackson EK, Menshikova EV, Mi Z, Verrier JD, Bansal R, Janesko-Feldman K, Jackson TC, Kochanek PM: Renal 2',3'-cyclic nucleotide 3'-phosphodiesterase is an important determinant of AKI severity after ischemia-reperfusion. *J Am Soc Nephrol* 27: 2069–2081, 2016
10. Yoshida T, Shimizu A, Masuda Y, Mii A, Fujita E, Yoshizaki K, Higo S, Kanzaki G, Kajimoto Y, Takano H, Fukuda Y: Caspase-3-independent internucleosomal DNA fragmentation in ischemic acute kidney injury. *Nephron Exp Nephrol* 120: e103–e113, 2012
11. Schumer M, Colombel MC, Sawczuk IS, Gobé G, Connor J, O'Toole KM, Olsson CA, Wise GJ, Buttyan R: Morphologic, biochemical, and molecular evidence of apoptosis during the reperfusion phase after brief periods of renal ischemia. *Am J Pathol* 140: 831–838, 1992
12. Ciccia A, Elledge SJ: The DNA damage response: Making it safe to play with knives. *Mol Cell* 40: 179–204, 2010
13. Harper JW, Elledge SJ: The DNA damage response: Ten years after. *Mol Cell* 28: 739–745, 2007
14. Jackson SP, Bartek J: The DNA-damage response in human biology and disease. *Nature* 461: 1071–1078, 2009
15. Hurley PJ, Bunz F: ATM and ATR: Components of an integrated circuit. *Cell Cycle* 6: 414–417, 2007
16. Sharma A, Singh K, Almasan A: Histone H2AX phosphorylation: A marker for DNA damage. *Methods Mol Biol* 920: 613–626, 2012
17. Tanaka T, Halicka D, Traganos F, Darzynkiewicz Z: Cytometric analysis of DNA damage: Phosphorylation of histone H2AX as a marker of DNA double-strand breaks (DSBs). *Methods Mol Biol* 523: 161–168, 2009
18. Chng SC, Ho L, Tian J, Reversade B: ELABELA: A hormone essential for heart development signals via the apelin receptor. *Dev Cell* 27: 672–680, 2013
19. Pauli A, Norris ML, Valen E, Chew GL, Gagnon JA, Zimmerman S, Mitchell A, Ma J, Dubrulle J, Reyon D, Tsai SQ, Joung JK, Saghatelian A, Schier AF: Toddler: An embryonic signal that promotes cell movement via Apelin receptors. *Science* 343: 1248636, 2014
20. Deng C, Chen H, Yang N, Feng Y, Hsueh AJ: Apela regulates fluid homeostasis by binding to the APJ receptor to activate Gi signaling. *J Biol Chem* 290: 18261–18268, 2015
21. Pastorino JG, Chen ST, Tafani M, Snyder JW, Farber JL: The overexpression of Bax produces cell death upon induction of the mitochondrial permeability transition. *J Biol Chem* 273: 7770–7775, 1998
22. Mello MB, Machado CS, Ribeiro DL, Aissa AF, Burim RV, Alves da Cunha MA, Barcelos GR, Antunes LM, Bianchi ML: Protective effects of the exopolysaccharide Lasiodiplodan against DNA damage and inflammation induced by doxorubicin in rats: Cytogenetic and gene expression assays. *Toxicology* 376: 66–74, 2017
23. Wondergem J, Stephens LC, Strebel FR, Baba H, Ohno S, Siddik ZH, Newman RA, Bull JM: Effect of adriamycin combined with whole body hyperthermia on tumor and normal tissues. *Cancer Res* 51: 3559–3567, 1991
24. Cao Q, Lu J, Li Q, Wang C, Wang XM, Lee VW, Wang C, Nguyen H, Zheng G, Zhao Y, Alexander SI, Wang Y, Harris DC: CD103+ dendritic cells elicit CD8+ T cell responses to accelerate kidney injury in adriamycin nephropathy. *J Am Soc Nephrol* 27: 1344–1360, 2016
25. Murza A, Besserer-Offroy É, Côté J, Bérubé P, Longpré JM, Dumaine R, Lesur O, Auger-Messier M, Leduc R, Sarret P, Marsault É: C-Terminal modifications of apelin-13 significantly change ligand binding, receptor signaling, and hypotensive action. *J Med Chem* 58: 2431–2440, 2015

26. Margathe JF, Iturrioz X, Alvear-Perez R, Marsol C, Riché S, Chabane H, Tounsi N, Kuhry M, Heissler D, Hibert M, Llorens-Cortes C, Bonnet D: Structure-activity relationship studies toward the discovery of selective apelin receptor agonists. *J Med Chem* 57: 2908–2919, 2014
27. Wang Z, Yu D, Wang M, Wang Q, Kouznetsova J, Yang R, Qian K, Wu W, Shuldiner A, Sztalryd C, Zou M, Zheng W, Gong DW: Elabela-apolin receptor signaling pathway is functional in mammalian systems. *Sci Rep* 5: 8170, 2015
28. Liu S, Hartleben B, Kretz O, Wiech T, Igarashi P, Mizushima N, Walz G, Huber TB: Autophagy plays a critical role in kidney tubule maintenance, aging and ischemia-reperfusion injury. *Autophagy* 8: 826–837, 2012
29. Kimura T, Takabatake Y, Takahashi A, Kaimori JY, Matsui I, Namba T, Kitamura H, Niimura F, Matsusaka T, Soga T, Rakugi H, Isaka Y: Autophagy protects the proximal tubule from degeneration and acute ischemic injury. *J Am Soc Nephrol* 22: 902–913, 2011
30. Wang W, Wang Q, Wan D, Sun Y, Wang L, Chen H, Liu C, Petersen RB, Li J, Xue W, Zheng L, Huang K: Histone HIST1H1C/H1.2 regulates autophagy in the development of diabetic retinopathy. *Autophagy* 2017: 1–14, 2017
31. Ho L, Tan SY, Wee S, Wu Y, Tan SJ, Ramakrishna NB, Chng SC, Nama S, Szczerbinska I, Chan YS, Avery S, Tsuneyoshi N, Ng HH, Gunaratne J, Dunn NR, Reversade B: ELABELA is an endogenous growth factor that sustains hESC self-renewal via the PI3K/AKT pathway. *Cell Stem Cell* 17: 435–447, 2015
32. Li M, Gou H, Tripathi BK, Huang J, Jiang S, Dubois W, Waybright T, Lei M, Shi J, Zhou M, Huang J: An Apela RNA-containing negative feedback loop regulates p53-mediated apoptosis in embryonic stem cells. *Cell Stem Cell* 16: 669–683, 2015
33. Tsuruya K, Furuichi M, Tominaga Y, Shinozaki M, Tokumoto M, Yoshimitsu T, Fukuda K, Kanai H, Hirakata H, Iida M, Nakabeppu Y: Accumulation of 8-oxoguanine in the cellular DNA and the alteration of the OGG1 expression during ischemia-reperfusion injury in the rat kidney. *DNA Repair (Amst)* 2: 211–229, 2003
34. Pabla N, Ma Z, McIlhatton MA, Fishel R, Dong Z: hMSH2 recruits ATR to DNA damage sites for activation during DNA damage-induced apoptosis. *J Biol Chem* 286: 10411–10418, 2011
35. Pabla N, Huang S, Mi QS, Daniel R, Dong Z: ATR-Chk2 signaling in p53 activation and DNA damage response during cisplatin-induced apoptosis. *J Biol Chem* 283: 6572–6583, 2008
36. Jiang M, Wei Q, Wang J, Du Q, Yu J, Zhang L, Dong Z: Regulation of PUMA-alpha by p53 in cisplatin-induced renal cell apoptosis. *Oncogene* 25: 4056–4066, 2006
37. Krüger K, Ziegler V, Hartmann C, Henninger C, Thomale J, Schupp N, Fritz G: Lovastatin prevents cisplatin-induced activation of pro-apoptotic DNA damage response (DDR) of renal tubular epithelial cells. *Toxicol Appl Pharmacol* 292: 103–114, 2016
38. Camano S, Lazaro A, Moreno-Gordaliza E, Torres AM, de Lucas C, Humanes B, Lazaro JA, Milagros Gomez-Gomez M, Bosca L, Tejedor A: Cilastatin attenuates cisplatin-induced proximal tubular cell damage. *J Pharmacol Exp Ther* 334: 419–429, 2010
39. Bonventre JV, Zuk A: Ischemic acute renal failure: An inflammatory disease? *Kidney Int* 66: 480–485, 2004
40. Abuelo JG: Normotensive ischemic acute renal failure. *N Engl J Med* 357: 797–805, 2007
41. Chen YT, Tsai TH, Yang CC, Sun CK, Chang LT, Chen HH, Chang CL, Sung PH, Zhen YY, Leu S, Chang HW, Chen YL, Yip HK: Exendin-4 and sitagliptin protect kidney from ischemia-reperfusion injury through suppressing oxidative stress and inflammatory reaction. *J Transl Med* 11: 270, 2013
42. Murza A, Sainsily X, Coquerel D, Côté J, Marx P, Besserer-Offroy É, Longpré JM, Lainé J, Reversade B, Salvail D, Leduc R, Dumaine R, Lesur O, Auger-Messier M, Sarret P, Marsault É: Discovery and structure-activity relationship of a bioactive fragment of ELABELA that modulates vascular and cardiac functions. *J Med Chem* 59: 2962–2972, 2016
43. Zhang X, Cheng B, Gong H, Li C, Chen H, Zheng L, Huang K: Porcine islet amyloid polypeptide fragments are refractory to amyloid formation. *FEBS Lett* 585: 71–77, 2011
44. Chen H, Li J, Jiao L, Petersen RB, Li J, Peng A, Zheng L, Huang K: Apelin inhibits the development of diabetic nephropathy by regulating histone acetylation in Akita mouse. *J Physiol* 592: 505–521, 2014
45. Sun Y, Xue W, Song Z, Huang K, Zheng L: Restoration of Opa1-long isoform inhibits retinal injury-induced neurodegeneration. *J Mol Med (Berl)* 94: 335–346, 2016
46. Li J, Huang J, Li JS, Chen H, Huang K, Zheng L: Accumulation of endoplasmic reticulum stress and lipogenesis in the liver through generational effects of high fat diets. *J Hepatol* 56: 900–907, 2012
47. Wang L, Li C, Guo H, Kern TS, Huang K, Zheng L: Curcumin inhibits neuronal and vascular degeneration in retina after ischemia and reperfusion injury. *Plos One* 6: e23194, 2011
48. Cai R, Xue W, Liu S, Petersen RB, Huang K, Zheng L: Overexpression of glyceraldehyde 3-phosphate dehydrogenase prevents neurovascular degeneration after retinal injury. *FASEB J* 29: 2749–2758, 2015
49. Chen H, Zheng C, Zhang X, Li J, Li J, Zheng L, Huang K: Apelin alleviates diabetes-associated endoplasmic reticulum stress in the pancreas of Akita mice. *Peptides* 32: 1634–1639, 2011
50. Huang J, Wan D, Li J, Chen H, Huang K, Zheng L: Histone acetyltransferase PCAF regulates inflammatory molecules in the development of renal injury. *Epigenetics* 10: 62–72, 2015
51. Ding Y, Li J, Liu S, Zhang L, Xiao H, Li J, Chen H, Petersen RB, Huang K, Zheng L: DNA hypomethylation of inflammation-associated genes in adipose tissue of female mice after multigenerational high fat diet feeding. *Int J Obes* 38: 198–204, 2014
52. Liu X, Zhou Y, Liu X, Peng A, Gong H, Huang L, Ji K, Petersen RB, Zheng L, Huang K: MPHOSPH1: A potential therapeutic target for hepatocellular carcinoma. *Cancer Res* 74: 6623–6634, 2014

This article contains supplemental material online at <http://jasn.asnjournals.org/lookup/suppl/doi:10.1681/ASN.2016111210/-/DCSupplemental>.